Nuclear Engineering and Technology 51 (2019) 1069–1074

Contents lists available at ScienceDirect

Nuclear Engineering and Technology

journal homepage: www.elsevier.com/locate/net

Original Article

A novel approach for manufacturing oxide dispersion strengthened (ODS) steel cladding tubes using cold spray technology

Benjamin Maier [a], Mia Lenling [a], Hwasung Yeom [a], Greg Johnson [a], Stuart Maloy [b], Kumar Sridharan [a, *]

[a] University of Wisconsin, Madison, WI, 53706, USA
[b] Los Alamos National Laboratory, Los Alamos, NM, 87545, USA

ARTICLE INFO

Article history:
Received 4 December 2018
Received in revised form
7 January 2019
Accepted 23 January 2019
Available online 24 January 2019

Keywords:
Oxide dispersion strengthened steel
14YWT powder
Cold spray process
ODS tube manufacturing

ABSTRACT

A novel fabrication method of oxide dispersion strengthened (ODS) steel cladding tubes for advanced fast reactors has been investigated using the cold spray powder-based materials deposition process. Cold spraying has the potential advantage for rapidly fabricating ODS cladding tubes in comparison with the conventional multi-step extrusion process. A gas atomized spherical 14YWT (Fe-14%Cr, 3%W, 0.4%Ti, 0.2% Y, 0.01%O) powder was sprayed on a rotating cylindrical 6061-T6 aluminum mandrel using nitrogen as the propellant gas. The powder lacked the oxygen content needed to precipitate the nanoclusters in ODS steel, therefore this work was intended to serve as a proof-of-concept study to demonstrate that free-standing steel cladding tubes with prototypical ODS composition could be manufactured using the cold spray process. The spray process produced an approximately 1-mm thick, dense 14YWT deposit on the aluminum-alloy tube. After surface polishing of the 14YWT deposit to obtain desired cladding thickness and surface roughness, the aluminum-alloy mandrel was dissolved in an alkaline medium to leave behind a free-standing ODS tube. The as-fabricated cladding tube was annealed at 1000 °C for 1 h in an argon atmosphere to improve the overall mechanical properties of the cladding.

1. Introduction

In-core structural components for nuclear reactors, such as fuel cladding for advanced fast reactors, operate in extreme environments of high temperatures (550–900 °C) and high radiation fields (damage levels of 10–150 dpa). Thus, it is desirable and in fact necessary that the structural materials deployed for fast reactor claddings have very good structural stability under high dose neutron irradiation (e.g., limited swelling) and good creep rupture strength at high temperatures [1]. Early development of fast reactor cladding materials focused on BCC ferritic/martensitic (FM) steels because of their radiation-induced swelling resistance up to neutron doses of 200 dpa and higher [2]. However, these materials typically do not exhibit sufficient creep rupture strength at temperatures higher than about 500 °C. In this regard, oxide dispersion strengthened (ODS) FM steels have received considerable attention because they provide a good combination of high temperature creep rupture strength and radiation damage resistance. ODS steels consist of a ferritic matrix with a uniform dispersion of Y-Ti-O nano-particles or nanoclusters which effectively pin dislocation motion at high temperatures [3]. ODS steels also exhibit good radiation damage resistance under neutron irradiation intrinsic to FM steels, and furthermore, the interfaces between the oxide nanoclusters and the FM matrix and high grain boundary density are believed to act as sinks for radiation-induced defects (e.g., void swelling) [4,5].

Current production of ODS cladding tubes is performed by a multiple step extrusion process, demonstrated, for example, in the paper by S. Ukai et al. [6] (see Fig. 1). In the scheme, the pre-alloyed ferritic matrix powders are first mechanically alloyed with the yttria powders under an argon gas atmosphere in an attrition ball mill for 48 h. Next, the powders are canned, degassed under vacuum, sealed, and then hot extruded at 1423 K. The cladding tubes are then cold rolled in a pilger mill and subsequently annealed at 1353 K. This step is repeated 6–10 times depending on the desired final dimensions. After the final cold rolling pass, depending on the dimensions, the tubes are either heat treated at 1373 K for 1 h or 1423 K for 60 s to strengthen the cladding tube through

* Corresponding author. Engineering Physics Department, 1500 Engineering Drive Rm. 919, University of Wisconsin, Madison, WI, 53706, USA.
E-mail address: kumar.sridharan@wisc.edu (K. Sridharan).

https://doi.org/10.1016/j.net.2019.01.015

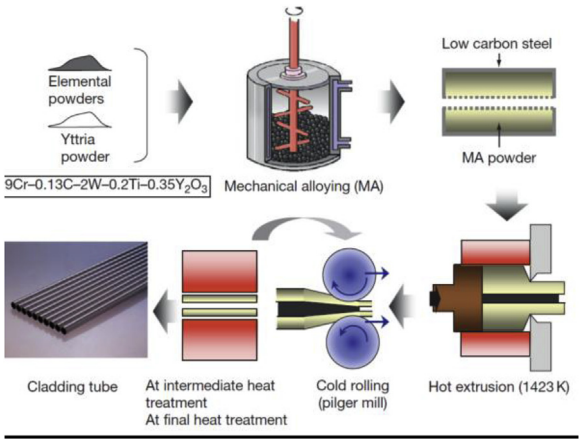

Fig. 1. Example of the typical steps involved in present manufacturing process of ODS steel cladding tubes (illustration from S. Ukai et al. [21]).

precipitation of the oxide nano-clusters. Subsequent surface finishing improvements such as polishing and sand blasting are then performed as a final manufacturing step [6]. This conventional manufacturing approach produces dimensionally accurate cladding tubes, while uniformly dispersing the oxide nano-clusters in the ferritic matrix. However, these multiple-step, low strain rate processes make the fabrication of the tubes expensive and time consuming. Another consequence of such conventional manufacturing approaches is that the tubes may develop anisotropic grains and, consequently, may have anisotropic mechanical properties [7]. To overcome the challenges, alternative manufacturing processes have been investigated. One example is the use of a laser beam scanning process to produce oxide dispersion strengthened (ODS) Zr-alloy. Here, a laser beam is scanned on the surface of a Y_2O_3 layer that is applied on the surface of a Zircaloy-4 substrate in order to induce a reaction between the Y_2O_3 and Zircaloy-4 to produce an ODS surface layer [8].

The research discussed here aims at manufacturing ODS cladding tubes using the cold spray additive manufacturing process. The cold spray process has the potential to obviate the large number of extrusion and annealing steps used in the present manufacturing approaches outlined earlier, and could offer a cost-effective approach for the manufacturing of ODS steel fuel claddings. Cold spray is a solid-state process which allows for fine microstructural control over the ODS steel material being deposited. Commonly studied additive manufacturing processes such as laser and electron beam methods involve melting which can lead to segregated microstructures making it difficult to control the microstructural properties. In particular, in the case of ODS steels, processes involving melting would lead to the upward stratification of oxide nanoparticles.

The cold spray process deposits materials at high velocities, at relatively low temperatures, and in a solid-state form. As shown in Fig. 2, the cold spray process operates by propelling powder particles of a material onto a substrate surface at supersonic velocities to form a neat-net shape component or coating. The particles are propelled via a high-velocity gas stream generated by the expansion of a pressurized, pre-heated gas through a converging-diverging nozzle. Bonding of particles occurs by plastic deformation and adiabatic shear mechanisms [9]. Since the particle deposition temperature is low, the original phase and compositional purity of the powder is preserved during the deposition process, and high-density, oxidation-free coatings or deposits can be achieved. Since cold spray is already a commercial process, it represents a viable alternative to the manufacturing of ODS steel fuel cladding tubes. The authors have recently developed the process for depositing oxidation-resistant coatings on Zr-alloy alloy LWR cladding for accident tolerant fuel [10,11].

The present research represents an initial feasibility study of the cold spray process for the manufacturing of ODS steel cladding tubes. Gas atomized 14YWT (Fe-14%Cr, 3%W, 0.4%Ti, 0.2%Y, 0.01%O) powder was used as the feedstock material to produce cladding tubes. It is noted that this powder lacked the oxygen content needed to precipitate oxide nanoclusters (>0.1 wt% oxygen is needed [12]) but was used to prove that cold spray could produce a high-quality, free-standing cladding tube with ODS ferritic matrix compositions. The feedstock powder was sprayed onto tube mandrel substrates, which were subsequently removed by a dissolution process to leave behind a free-standing ODS steel tube. The cladding tube was then annealed for stress relief, recrystallization, and for enhancing the ductility of the cladding.

2. Experimental procedure

The ODS steel powder for this cladding manufacturing study was supplied by Los Alamos National Laboratory but originally produced by ATI Powder Metals (Pittsburgh, PA). The powder received was −325 mesh, gas atomized 14YWT with a composition of (Fe-14%Cr, 3%W, 0.4%Ti, 0.2%Y, 0.01%O). Commercial 5083-H116 Al alloy flats were purchased from Sunshine Metals (Harvey, LA) along with 4130 annealed steel flat substrates from Online Metals (Seattle, WA). These flats were used as substrates for initial demonstration of cold spray deposition of the powder (e.g., flowability and deposition efficiency). Cylindrical tubes of 6061-T6 aluminum (9.525 mm O.D.) were also procured as substrate mandrels to demonstrate the manufacturability of 14YWT cladding tubing using the cold spray deposition process. Prior to deposition, the aluminum-alloy substrates (flats and tubes) were ground with 320-grit SiC abrasive paper and the steel substrate flats were grit blasted with 36-grit alumina in order to improve adhesion of the deposited material on the substrates. The substrates were then thoroughly cleaned using ethanol to minimize contamination at the surface that may adversely affect the subsequent deposition.

Cold spray deposition was performed using a commercial Cold Gas Kinetiks 4000/34 unit system (Ampfing, Germany) with a Type 24 converging-diverging De Laval type tungsten carbide nozzle. The gas preheat temperature was 800 °C, pressure was 35 bar, and distance from the gun to the substrate (stand-off distance) was 26 mm. A Sherline lathe (Vista, California) holding the aluminum tubing was rotated at 400 rpm and the gun traverse speed was 3.3 mm/s axially over the rotating tubing for a total of two passes. The gun was aligned directly over the center of the tubing to ensure maximum deposition. The flat substrates were mounted on a vertical sample holder. A Nachi system robot from Antenen (West Chester, OH) was used to support the spray gun so that precise movements of the gun could be programmed. The gun and spray system were enclosed in a spray booth from Noise Barriers (Libertyville, IL) in order to minimize the noise, confine the undeposited powder, and exhaust the spent gas. Industrial grade (certified 99.998% purity) nitrogen was used as the propellant gas.

After spraying, the mandrel tube substrate was dissolved using an aqueous 20% NaOH solution over 20 h to completely remove all of the aluminum alloy and leave a free-standing ODS tube. A subsequent heat treatment was then performed in a quartz tube filled with Ar at 1000 °C for 1 h to induce recrystallization and potentially enhance ductility.

A Zeiss LEO Scanning Electron Microscope (SEM) was used for characterization of the powder size and morphology as well as the thickness and microstructure of the deposits. Energy Dispersive Spectroscopy (EDS) was used to examine the powder chemistry and

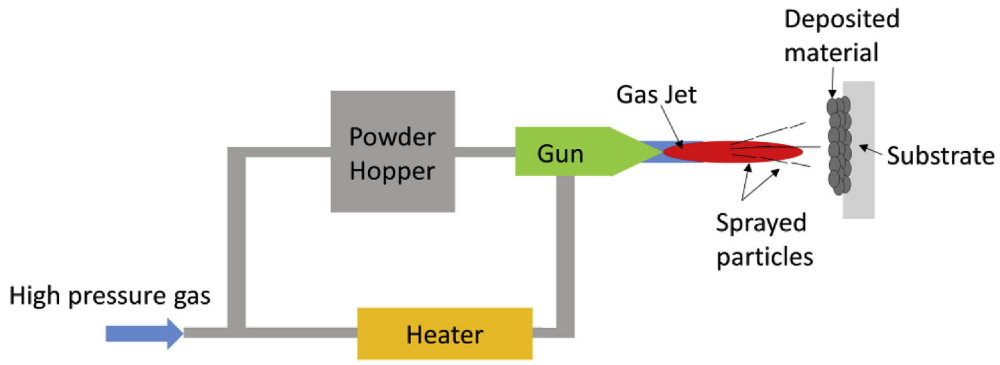

Fig. 2. Schematic illustration of the cold spray process being investigated in this study.

potential yttrium segregation in the powders. A Bruker D8 Discovery x-ray diffractometer (XRD) with a Cu Kα radiation source from a 2θ range of 30°–90° was used to identify the phases in both the powders and the deposits. Knoop microhardness was performed as a measure of the microstructural changes induced from annealing, using a 25 g load on the as-deposited ODS cladding and annealed ODS cladding.

3. Results and discussion

Gas atomized 14YWT (Fe-14%Cr, 3%W, 0.4%Ti, 0.2%Y, 0.01%O) was used as the cold spray feedstock material. This powder was manufactured by alloying yttrium and titanium in molten ferritic steel followed by gas atomization to produce spherical powder. The high cooling rates experienced by the molten droplets promotes solute trapping and incorporation of Y and Ti in solid solution. As mentioned previously, oxygen content in the powder was low, and therefore not conducive for the precipitation of the oxide nanoclusters inherent to ODS steels. This powder was therefore used for proof-of-concept that a cladding tube could be produced by the cold spray process. SEM of the powder showed a spherical morphology with powders ranging in size from 5 to 44 μm as shown in Fig. 3a. Spherical powder morphology is ideal for cold spray so that good powder flowability in mechanical type powder feeders can be achieved [13]. The powders were sieved into size ranges, 20 μm to 44 μm and less than 20 μm, following which powders from each size range were mounted and polished in cross-section for microstructural examination. The cross-sectional SEM images of powders of the two size ranges are shown in Fig. 3b and c. In general, powders of both sizes exhibited cellular equiaxed grains typical of atomized powders.

Compositional analysis of several particles using EDS point measurements suggested that despite the high cooling rate during atomization, yttrium segregation is observed in certain regions of the particles, particularly in the vicinity of the grain boundaries. However as shown in Fig. 4, fewer yttrium segregation events were observed in the smaller particles likely due to the higher cooling rates experienced by the smaller particles, which promoted solute trapping. Therefore, it is likely that yttrium was not homogenously solutionized in the powder particles. Nevertheless, this does not affect the goal of demonstrating the manufacturing of cladding tubes of ODS steel compositions using the cold spray process.

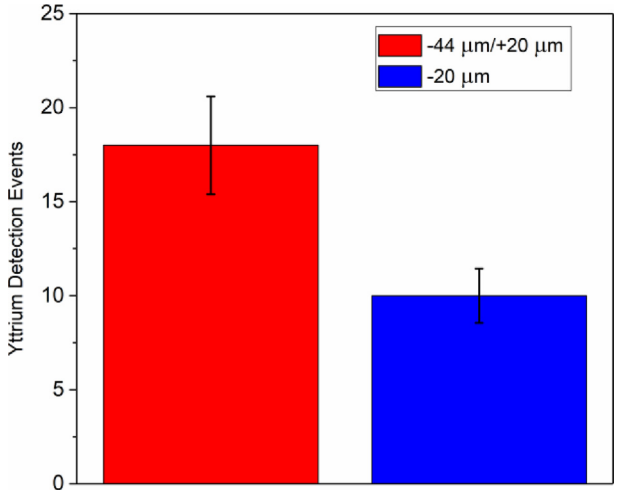

Fig. 4. Number of yttrium detection events from point scan EDS analysis for the two particle size ranges.

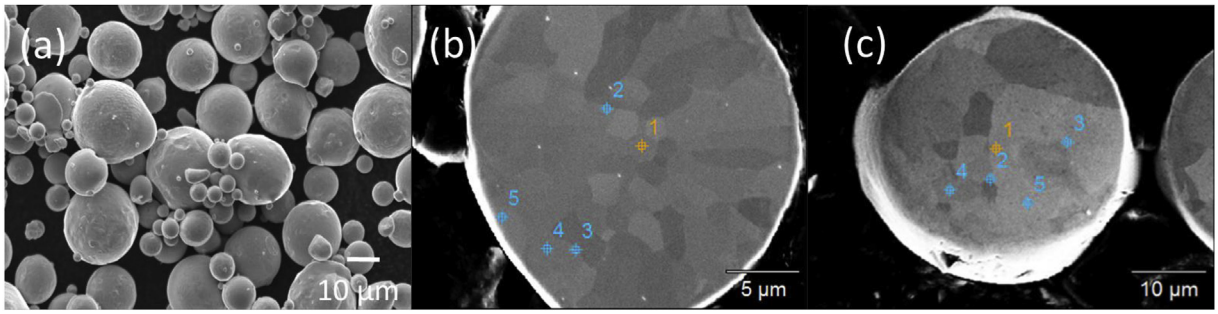

Fig. 3. SEM micrographs of the gas atomized 14YWT ODS powder in (a) as-received powders showing a range of powder particle sizes (b) cross-section image of powder from the <20 μm size range, (c) cross-section image of powder from the 20 μm–44 μm size range. The cross-sectional images also indicate the points where EDS analysis was performed for data for shown in Fig. 4.

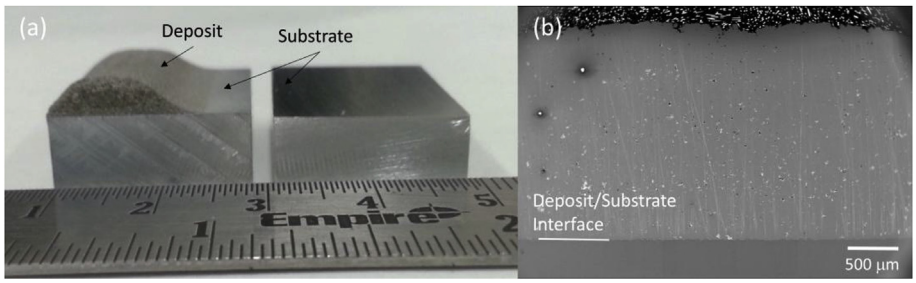

Fig. 5. Initial 14YWT powder deposition results, (a) photograph of as-deposited 14YWT powder on 5083 aluminum alloy flat and (b) cross-sectional SEM image of the as-deposited material.

Previous work has shown that this segregation can be largely eliminated using mechanical alloying to homogenize the constituent elements [14].

Initial deposition of the 14YWT powder was successful on both the 5083 aluminum-alloy and 4130 steel flats. A deposit thickness of well above 2 mm was achieved on both substrate materials as shown in Fig. 5. Even though deposition was achieved on both flats, an aluminum alloy (6061-T6) was chosen as the substrate for actual tube fabrication based on the ability to be able to dissolve aluminum-alloys in alkaline solutions such as NaOH. XRD was then performed on the 14YWT powder and deposit to quantify phase changes, or lack thereof, during the cold spray process. Fig. 6 shows that the phase purity of the powder was retained in the deposit and no second phases formed; a natural advantage of the low temperature, solid-state deposition of the cold spray process.

The 14YWT powder was then deposited onto a 6061-T6 aluminum alloy tube mandrel substrate using the knowledge of spray parameters derived from spraying flat geometries. The deposition was accomplished by spraying onto a tube rotated about its longitudinal axis and a 1 mm deposition thickness was achieved. The thickness of the deposit was reduced to 0.8 mm by polishing

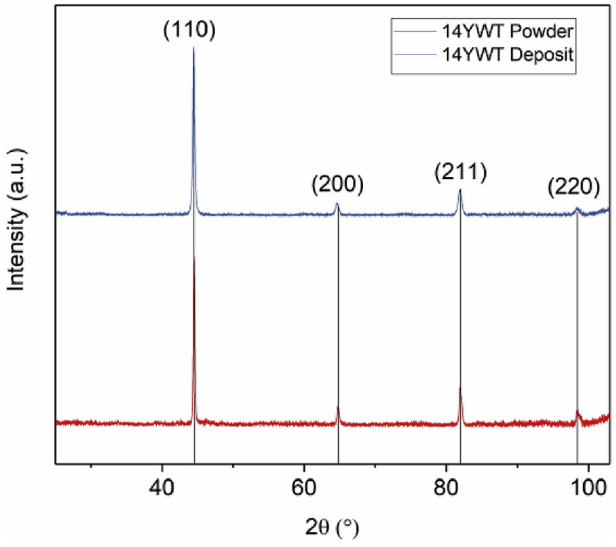

Fig. 6. XRD patterns of the 14YWT ODS powder and cold spray deposit of this material confirming that phase and compositional purity was retained during deposition.

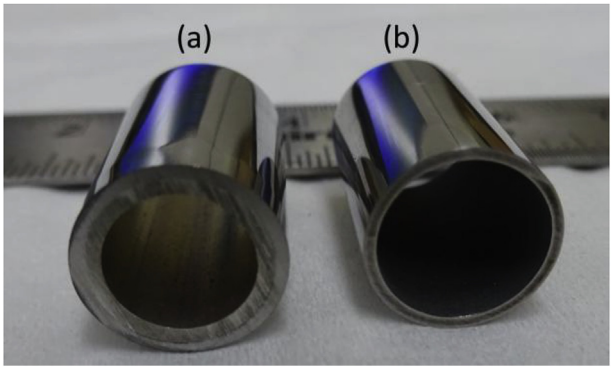

Fig. 8. Photograph of 14YWT ODS tube after surface polishing showing (a) ODS deposit with the 6061-T6 Al-alloy substrate tube, and (b) after dissolution of the inner Al-alloy substrate tube showing free standing ODS tube.

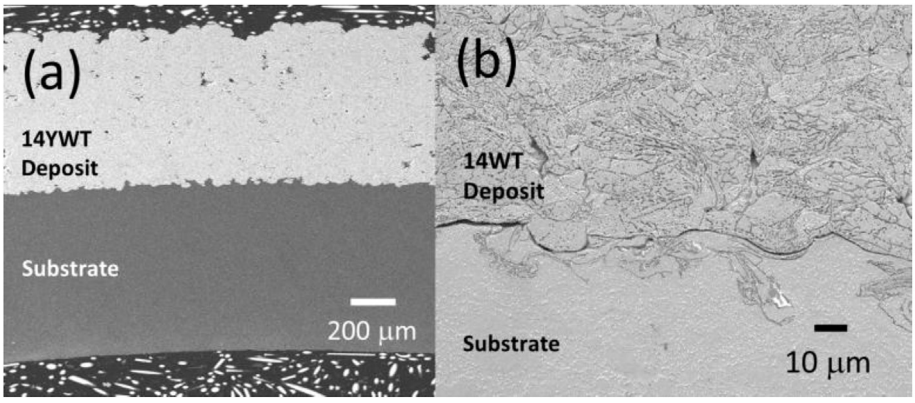

Fig. 7. Cross-sectional SEM image of tubular deposition of 14YWT (a) showing deposition on tubular mandrel substrate (b) high magnification image of deposit and substrate interface after etching with Kalling's reagent.

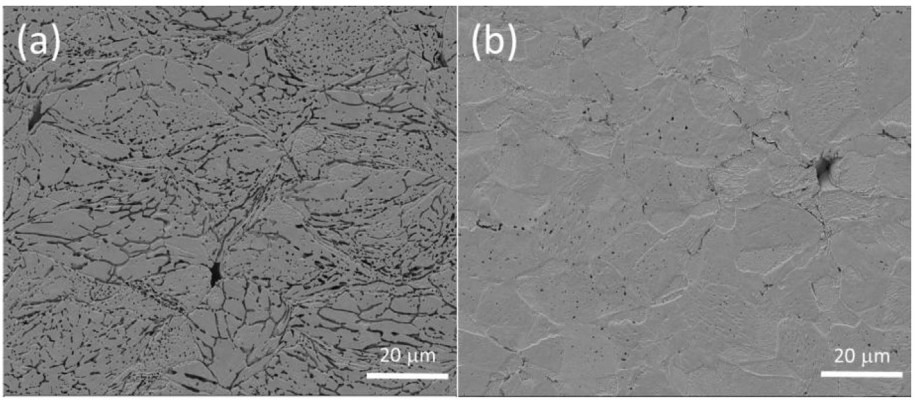

Fig. 9. Etched microstructure of ODS cladding (a) before annealing and (b) after annealing at 1000 °C for 1 h.

the tube surface while rotating it in the lathe – this thickness was selected based on general nuclear reactor cladding wall thicknesses. However, for fast reactors this cladding wall thickness may be a bit smaller. Cross-sectional SEM of the tubular deposit on the substrate is shown in Fig. 7a, while Fig. 7b shows a higher magnification etched image of the deposit. Inter-particle boundaries (IPBs) were observed after etching and the lack of clarity in the microstructure in the etched sample is attributed to severe deformation effects in the deposit. Knoop microhardness was also measured according to the ASTM E384 standard [15] and an average value of 325 H_K was obtained.

As mentioned previously, the deposit surface was progressively ground starting with 320 grit up to a final polish with 800 grit SiC paper to decrease the surface roughness and thickness. The deposit substrate system after polishing is shown in the photograph in Fig. 8a, revealing a lustrous metallic surface. The aluminum alloy substrate was then dissolved using a 20% NaOH solution [16] over a 20 h period. The final, free standing ODS steel cladding is shown in Fig. 8b.

Annealing of the cladding was performed at 1000 °C for 1 h in argon atmosphere with the goal of inducing recrystallization and promoting ductility. In actual ODS compositions, that contain sufficient Y, Ti, and O, such a treatment is essential for the precipitation of (Y, Ti)-O nanoclusters which impart the outstanding properties to the ODS steel [17,18]. A comparison of Fig. 9a and b suggests that annealing resulted in the formation of more equiaxed grains and elimination of inter-particle boundaries which represent manifestations of anisotropy. The hardness value dropped to 279 $H_K \pm 28$ due to recrystallization, and the porosity of the annealed product was less than 0.5%. The hardness decrease is expected to improve the ductility of the cladding [19]. Since it is known that microhardness values vary linearly with tensile strength [20], it can be concluded with reasonable confidence that the tensile strength of the ODS deposits decreased after the annealing treatment. Literature values for the hardness of ODS cladding tubes under the conventional manufacturing process after annealing have been reported to be about 350 H_K due to the formation of oxide nanoclusters in the size range of 2–4 nm which pin dislocations [19]. The lower hardness of the steels produced in the present study may be due to the absence of these oxide nanoclusters because of insufficient oxygen in the feedstock powder particle matrix. However, future work by the authors will focus on higher oxygen-containing steels and the identification, analysis, and quantification of oxide nanoclusters using high-resolution Transmission Electron Microscopy. High temperature mechanical tests will also be performed in the future.

4. Conclusions

ODS steel cladding tubes have been successfully fabricated using the cold spray deposition process in a near-net shape manufacturing approach. First, 14YWT powder was deposited using the cold spray process onto a rotating cylindrical 6061-T6 aluminum tube mandrel, to a thickness slightly in excess of the intended cladding wall thickness. The powders lacked the oxygen content needed to precipitate oxide nanoclusters but effectively demonstrated that the cold spray process could produce a high-quality, free-standing cladding tube at near theoretical density with a ferritic microstructure and metal-composition corresponding to ODS alloys. The surface of the deposit was polished and the aluminum-alloy substrate mandrel tube was subsequently removed by dissolution in an alkaline solution. The free-standing 14YWT tube was then heat treated at 1000 °C for 1 h to anneal and densify the deposit. The technique has the potential to obviate the need for multiple extrusion and annealing steps presently used for fabricating ODS steel cladding tubes, and provides a rapid, cost-effective method for manufacturing such tubes.

Acknowledgements

This work was supported by the U.S. Department of Energy Grant No. DE-NE0008682 and by the National Academics Keck Future Initiative (National Academy of Sciences) grant NAKFI ANT10.

Appendix A. Supplementary data

Supplementary data to this article can be found online at https://doi.org/10.1016/j.net.2019.01.015.

References

[1] K.L. Murty, I. Charit, Structural materials for Gen-IV nuclear reactors: challenges and opportunities, J. Nucl. Mater. 383 (2008) 189–195.
[2] A. Kohyama, A. Hishinuma, D.S. Gelles, R.L. Klueh, W. Dietz, K. Ehrlich, Low-activation ferritic and martensitic steels for fusion application, J. Nucl. Mater. 233–237 (1996) 138–147.
[3] R.L. Klueh, J.P. Shingledecker, R.W. Swindeman, D.T. Hoelzer, Oxide dispersion-strengthened steels: a comparison of some commercial and experimental alloys, J. Nucl. Mater. 341 (2005) 103–114.
[4] V. Sagaradze, V. Shalaev, V. Arbuzov, B. Goshchitskii, Y. Tian, W. Qun, S. Jiguang, Radiation resistance and thermal creep of ODS ferritic steels, J. Nucl. Mater. 295 (2001) 265–272.
[5] D.A. McClintock, M.A. Sokolov, D.T. Hoelzer, R.K. Nanstad, Mechanical properties of irradiated ODS-EUROFER and nanocluster strengthened 14YWT, J. Nucl. Mater. 392 (2009) 353–359.
[6] S. Ukai, T. Yoshitake, S. Mizuta, Y. Matsudaira, S. Hagi, T. Kobayashi,

Preliminary tube manufacturing of oxide dispersion strengthened ferritic steels with recrystallized structure, J. Nucl. Sci. Technol. 36 (1999) 710–712.
[7] A. Alamo, H. Regle, G. Pons, J.L. Béchade, Microstructure and textures of ods ferritic alloys obtained by mechanical alloying, Mater. Sci. Forum 88–90 (1992) 183–190.
[8] H.-G. Kim, I.-H. Kim, Y.-I. Jung, D.-J. Park, J.-H. Park, J.-H. Yang, Y.-H. Koo, Microstructure and mechanical characteristics of surface oxide dispersion-strengthened Zircaloy-4 cladding tube, Addit. Manuf. 22 (2018) 75–85.
[9] V.K. Champagne, The Cold Spray Materials Deposition Process : Fundamentals and Applications, Woodhead, 2007.
[10] H. Yeom, B. Maier, G. Johnson, T. Dabney, J. Walters, K. Sridharan, Development of cold spray process for oxidation-resistant FeCrAl and Mo diffusion barrier coatings on optimized ZIRLO™, J. Nucl. Mater. 507 (2018) 306–315.
[11] B. Maier, H. Yeom, G. Johnson, T. Dabney, J. Walters, J. Romero, H. Shah, P. Xu, K. Sridharan, Development of cold spray coatings for accident-tolerant fuel cladding in light water reactors, JOM 70 (2018) 198–202.
[12] G.R. Odette, Recent progress in developing and qualifying nanostructured ferritic alloys for advanced fission and fusion applications, JOM 66 (2014) 2427–2441.
[13] S.V. Klinkov, V.F. Kosarev, M. Rein, Cold spray deposition: significance of particle impact phenomena, Aero. Sci. Technol. 9 (2005) 582–591.
[14] D.T. Hoelzer, J. Bentley, M.A. Sokolov, M.K. Miller, G.R. Odette, M.J. Alinger, Influence of Particle Dispersions on the High-Temperature Strength of Ferritic Alloys, (n.d.).
[15] Standard Test Method for Microindentation Hardness of Materials 1, ASTM Int. (n.d.).
[16] Sample Dissolution, ASM Handb, Vol. 10, 1986, pp. 161–180.
[17] M.K. Miller, K.F. Russell, D.T. Hoelzer, Characterization of precipitates in MA/ODS ferritic alloys, J. Nucl. Mater. 351 (2006) 261–268.
[18] M.K. Miller, D.T. Hoelzer, E.A. Kenik, K.F. Russell, Stability of ferritic MA/ODS alloys at high temperatures, Intermetallics 13 (2005) 387–392.
[19] H.L. Ding, R. Gao, T. Zhang, X.P. Wang, Q.F. Fang, C.S. Liu, Annealing effect on the microstructure and magnetic properties of 14%Cr-ODS ferritic steel, Fusion Eng. Des. 100 (2015) 371–377.
[20] E.J. Pavlina, C.J. Van Tyne, Correlation of yield strength and tensile strength with hardness for steels, J. Mater. Eng. Perform. 17 (2008) 888–893.
[21] S. Ukai, M. Harada, H. Okada, M. Inoue, S. Nomura, S. Shikakura, T. Nishida, M. Fujiwara, K. Asabe, Tube manufacturing and mechanical properties of oxide dispersion strengthened ferritic steel, J. Nucl. Mater. 204 (1993) 74–80.